Aerosol Science and Technology 36: 318–328 (2002)

Published by Taylor and Francis
0278-6826/02/$12.00 + .00

The Macroscopic Effects of Internal and External Electric Fields on Profile and Thermodynamics of a Dielectric Droplet

A. K. Shchekin, M. S. Kshevetskiy, and V. B. Warshavsky
Department of Statistical Physics, Research Institute of Physics, St. Petersburg State University, Petrodvoretz, Russia

The effects of weak and strong axisymmetric electric fields on the profile and thermodynamic characteristics of a dielectric droplet in the vapor-gas environment have been considered. The procedure for numerical solution of the coupled nonlinear equations for the equilibrium droplet shape and the electric field potential has been illustrated in the case of an external uniform electric field and the case of a nonuniform internal field of the heterogeneous nucleus with an electric dipole moment. Analytical results of perturbation theory for small nonspherical deformations in the droplet shape and surface area have been shown to be really limited to small electric field effects. However, the analytical results for the chemical potential and free energy of droplet formation (which are of first importance for nucleation phenomena and liquid aerosol formation in a gaseous atmosphere) are valid even for rather strong fields due to mutual compensation between the nonspherical contribution to the surface area and the contribution due to droplet polarization.

INTRODUCTION

An electric field is able to significantly affect the thermodynamics and kinetics of liquid aerosol formation. The good example is ion-induced nucleation when a droplet is formed in a strong central electric field of ion and the field considerably reduces the critical vapor supersaturation (Wilson 1900; Holland and Castleman 1982). In addition, if the electric field is noncentral (as in the case of an external field, the field of a condensation nucleus with a dipole moment, or ion-induced nucleation in an external field), the equilibrium droplet shape becomes nonspherical and an instability of droplets may be invoked. Effects of an electric field in nucleation appear mainly through variation of the characteristic thermodynamic quantities of aerosol droplets: the chemical potential of condensate in nucleating droplets or the work of droplet formation (Kuni et al. 1984; Cheng 1984). One can expect that the effects in the case of the external field are weak for small subcritical or critical droplets in nucleation, but can be nonlinear for supercritical drops. By contrast, the role of the internal field of the condensation nucleus should be larger for very small subcritical nucleating droplets.

The distortion of the equilibrium droplet shape in the case of a strong noncentral field impedes analytical findings of thermodynamic quantities of nucleation, except for the case of ellipsoidal droplets in the uniform external field (Cheng 1984; Cheng and Chaddock 1984). In order to find the chemical potential of condensate in nucleating droplets or the work of droplet formation in a strong axisymmetric field, we need a reliable approach allowing simultaneous solving of the coupled nonlinear equations for the equilibrium droplet shape and the electric field potential. Such an approach to computing the equilibrium shape of conducting and dielectric drops in the uniform external electric field was proposed in Basaran and Scriven (1989) and Wohlhuter and Basaran (1993). Nevertheless, neither the thermodynamic characteristics of the drops relevant for nucleation theory nor the effects of the internal nonuniform nonspherical electric field were considered. In this paper we present a numerical scheme for analysis of the effects of an arbitrary axisymmetric electric field on the equilibrium shape of a dielectric droplet and thermodynamic characteristics of nucleation of such droplets. We compare the results of this approach with the analytical results obtained previously in the cases of the external uniform electric field (Cheng 1984; Cheng and Chaddock 1984; Warshavsky and Shchekin 1996, 1999) and the nonuniform internal field of the heterogeneous condensation nucleus with an electric dipole moment (Shchekin and Varshavskii 1996).

Received 14 August 2000; accepted 10 April 2001.
Alexander Shchekin thanks the Program "Universities of Russia—basic Research" (project no. 992809). Vadim Warshavsky and Mikhail Kshevetskiy thank the Euler Program (Freie Universität Berlin) for the financial support of this work.
Address correspondence to A. K. Shchekin, Department of Statistical Physics, Research Institute of Physics, St. Petersburg State University, Ulyanovskaya 1, Petrodvoretz, 198504 Russia. E-mail: Alexander.Shchekin@pobox.spbu.ru

BASIC EQUATIONS

Let us consider a droplet (with volume V) condensing out of the vapor-gas environment (phase β) in the electric field. The source of the electric field may be located outside or inside the droplet (as in the case of the droplet formed on a heterogeneous condensation nucleus). Let the droplet consist of ν molecules of an incompressible liquid dielectric (phase α). Hereafter, the indices α and β denote the quantities referred to as the liquid and the vapor phase, respectively. Only one component in these phases is condensable. The effect of the gravity on the droplet is assumed to be negligible as well as the effects of the electric double layer at the droplet surface. First we will consider the droplet in full equilibrium, which corresponds to the extreme point in the work of droplet formation at a given vapor supersaturation, but the results can be extended (Kuni et al. 1984; Shchekin and Varshavskii 1996) for all droplets relevant for nucleation.

The number ν determines the size of the droplet. The balance of local pressures at any point on the droplet surface governs the equilibrium shape of a droplet:

$$P_N^\alpha - P_N^\beta - P_\gamma = 0, \qquad [1]$$

where

$$P_N^\alpha = P_0^\alpha - \sigma_N^\alpha, \qquad P_N^\beta = P_0^\beta - \sigma_N^\beta, \qquad [2]$$

P_0 is the pressure in a phase in absence of the electric field, σ_N is the normal component of the Maxwell stress tensor, and P_γ is the capillary pressure under the curved droplet surface. If the thickness of the droplet surface layer is small enough in comparison to the droplet size, we can consider the surface tension γ as the scalar quantity independent of droplet size and write

$$P_\gamma = \gamma\left(\frac{1}{R_1} + \frac{1}{R_2}\right). \qquad [3]$$

Here R_1 and R_2 are the principal radii of the surface curvature at any point on the droplet surface where the local pressure balance (1) holds. If we fix the chemical potential of the droplet substance in absence and presence of the electric field, i.e., pressure P_0 is determined at the same chemical potential μ as in the presence of the electric field, then we have

$$\sigma_N = \varepsilon(\mu)\frac{(\vec{E},\vec{n})^2}{4\pi} - \varepsilon(\mu)\frac{(\vec{E})^2}{8\pi}, \qquad [4]$$

where $\varepsilon(\mu)$ is the dielectric permittivity determined as a function of chemical potential μ, $\vec{E}$ is the vector of the electric field intensity, and $\vec{n}$ is the unit vector of the outer normal to the droplet surface.

Let us assume the axial symmetry of the electric field. Choosing the spherical coordinate system with the center at the droplet mass center and the polar axis directed along the vector $\vec{E}$, evaluating the sum of principal curvatures in (3), we obtain

$$P_\gamma = \frac{\gamma}{\sqrt{r^2+(1-x^2)r_x^2}}\left[2 + \frac{(1-x^2)\left(r_x^2 - rr_{xx}\right)+xrr_x}{r^2+(1-x^2)r_x^2} + \frac{xr_x}{r}\right], \qquad [5]$$

while the expression for unit vector of the outer normal $\vec{n}$ has the form

$$\vec{n} = \frac{r\vec{e}_r - r_x\sqrt{1-x^2}\vec{e}_\theta}{\sqrt{r^2+(1-x^2)r_x^2}}. \qquad [6]$$

Here $x \equiv \cos\theta$, θ is the polar angle between the polar axis and the radius vector $\vec{r}'$ of the observation point, $r(\theta) \equiv r(x)$ is the droplet profile, $r_x \equiv dr/dx$, $r_{xx} \equiv d^2r/dx^2$, and $\vec{e}_r$ and $\vec{e}_\theta$ are the unit vectors in the radial and the azimuthal directions.

The electric field intensity $\vec{E}$ is related to electric potential $\Phi(r', x)$ as $\vec{E} \equiv -\nabla\Phi$. In order to determine $\Phi^\alpha(r', x)$ and $\Phi^\beta(r', x)$, we need to solve the Laplace equations

$$\Delta\Phi^\alpha = 0 \quad \text{and} \quad \Delta\Phi^\beta = 0 \qquad [7]$$

with the standard boundary conditions at the droplet surface,

$$\Phi^\alpha|_{r'=r(x)} = \Phi^\beta|_{r'=r(x)}, \qquad [8]$$

$$\varepsilon^\alpha(\mu)(\nabla\Phi^\alpha, \vec{n})|_{r'=r(x)} = \varepsilon^\beta(\mu)(\nabla\Phi^\beta, \vec{n})|_{r'=r(x)}, \qquad [9]$$

and the specific boundary conditions at the locations of field sources. In the case of the external uniform electric field and in the case of the internal nonuniform electric field of a heterogeneous condensation nucleus with a dipole moment we have, respectively,

$$\Phi^\alpha|_{r'=0} = const, \qquad \Phi^\beta \underset{r'\to\infty}{\longrightarrow} -E_\infty r' x, \qquad [10a]$$

$$\Phi^\alpha \underset{r'\to 0}{\longrightarrow} \frac{px}{\varepsilon^\alpha(\mu)r'^2}, \qquad \Phi^\beta \underset{r'\to\infty}{\longrightarrow} 0, \qquad [10b]$$

where E_∞ is the absolute magnitude of the external electric field intensity as $r' \to \infty$ and p is the electric dipole moment of the heterogeneous condensation nucleus.

In view of Equations (2)–(6), (8), and (9), we can rewrite the balance Equation (1) as an ordinary nonlinear differential equation for the droplet profile $r(x)$,

$$\frac{\gamma}{\sqrt{r^2+(1-x^2)r_x^2}}\left[2 + \frac{(1-x^2)\left(r_x^2 - rr_{xx}\right)+xrr_x}{r^2+(1-x^2)r_x^2} + \frac{xr_x}{r}\right] - \frac{\varepsilon^\alpha(\mu)-\varepsilon^\beta(\mu)}{8\pi} \times\left[\frac{\left(r^2\Phi_r^\alpha - (1-x^2)r_x\Phi_x^\alpha\right)\left(r^2\Phi_r^\beta - (1-x^2)r_x\Phi_x^\beta\right)}{r^2\left(r^2+(1-x^2)r_x^2\right)} + \frac{(1-x^2)\left(\Phi_x^\alpha + r_x\Phi_r^\alpha\right)\left(\Phi_x^\beta + r_x\Phi_r^\beta\right)}{r^2+(1-x^2)r_x^2}\right] - P_0^\alpha + P_0^\beta = 0, \qquad [11]$$

where $\Phi_r \equiv \partial\Phi/\partial r'|_{r'=r(x)}$, $\Phi_x \equiv \partial\Phi/\partial x|_{r'=r(x)}$.

As was shown in Warshavsky and Shchekin (1996, 1999) and Shchekin and Varshavskii (1996), the solution of Equation (11) simultaneously with Equation (7) allows us to find not only

the droplet profile $r(\theta)$ and the electric potentials Φ^α and Φ^β, but also the thermodynamic droplet characteristics relevant for nucleation and, first of all, the chemical potential of condensate in the nucleating droplet. Because the number of condensate molecules evaporating out of droplet per unit time is a function of the chemical potential of condensate, finding the condensate chemical potential in the droplet means also that the influence of the electric field on the evaporation of the droplet is described.

THE CHARACTERISTIC SCALES AND INDEPENDENT PARAMETERS

Let us define the characteristic scales for the problem. Let R be the radius of the equivalent sphere for the droplet, i.e., the sphere with the same volume as the volume of the droplet, Ψ be the characteristic electric potential (which depends on boundary conditions and will be specified later), $4\pi\gamma R^2$ be the characteristic surface energy, and $\varepsilon \equiv \varepsilon^\alpha(\mu)/\varepsilon(\mu)$ be the relative dielectric permittivity. Introducing these scales into Equations (7)–(9) and (11), we can determine dimensionless quantities $g_i, i = 1, 2, 3$, as

$$g_1(x) \equiv \tilde{\Phi}^\alpha(\tilde{r}(x), x) - \tilde{\Phi}^\beta(\tilde{r}(x), x), \qquad [12]$$

$$g_2(x) \equiv \varepsilon\left(\tilde{r}^2\tilde{\Phi}^\alpha_r - (1-x^2)\tilde{r}_x\tilde{\Phi}^\alpha_x\right) - \left(\tilde{r}^2\tilde{\Phi}^\beta_r - (1-x^2)\tilde{r}_x\tilde{\Phi}^\beta_x\right), \qquad [13]$$

$$\begin{aligned} g_3(x) &\equiv -G + \frac{1}{2\sqrt{\tilde{r}^2 + (1-x^2)\tilde{r}_x^2}} \\ &\times \left[2 + \frac{(1-x^2)\left(\tilde{r}_x^2 - \tilde{r}\tilde{r}_{xx}\right) + x\tilde{r}\tilde{r}_x}{\tilde{r}^2 + (1-x^2)\tilde{r}_x^2} + \frac{x\tilde{r}_x}{\tilde{r}}\right] \\ &- H^2\left[\frac{\left(\tilde{r}^2\tilde{\Phi}^\alpha_r - (1-x^2)\tilde{r}_x\tilde{\Phi}^\alpha_x\right)\left(\tilde{r}^2\tilde{\Phi}^\beta_r - (1-x^2)\tilde{r}_x\tilde{\Phi}^\beta_x\right)}{\tilde{r}^2\left(\tilde{r}^2 + (1-x^2)\tilde{r}_x^2\right)}\right. \\ &\left. + \frac{(1-x^2)\left(\tilde{\Phi}^\alpha_x + \tilde{r}_x\tilde{\Phi}^\alpha_r\right)\left(\tilde{\Phi}^\beta_x + \tilde{r}_x\tilde{\Phi}^\beta_r\right)}{\tilde{r}^2 + (1-x^2)\tilde{r}_x^2}\right]. \end{aligned} \qquad [14]$$

Here

$$G \equiv \frac{P_0^\alpha - P_0^\beta}{2\gamma}R, \qquad [15]$$

$$H^2 \equiv \frac{\Psi^2(\varepsilon^\alpha(\mu) - \varepsilon^\beta(\mu))}{16\pi\gamma R}, \qquad [16]$$

the tilde marks the dimensionless quantities: $\tilde{r} \equiv r/R$, $\tilde{\Phi} \equiv \Phi/\Psi$, and, as follows from the definition of radius R,

$$\int_{-1}^{1} dx\tilde{r}^3(x) = 2. \qquad [17]$$

We can consider G as the dimensionless chemical potential of condensate in the droplet. The meaning of H depends on the specific choice of the potential Ψ. If we choose the scale potential Ψ in the case of boundary conditions (10a) and (10b) as

$$\Psi \equiv E_\infty R \qquad [18a]$$

and

$$\Psi \equiv p/\varepsilon^\alpha(\mu)R^2, \qquad [18b]$$

respectively, the dimensionless parameter H can be determined as

$$H = \sqrt{\frac{(\varepsilon^\alpha(\mu) - \varepsilon^\beta(\mu))R}{16\pi\gamma}}E_\infty \qquad [19a]$$

(H has the meaning of the dimensionless intensity of the external electric field) and

$$H = \sqrt{\frac{(\varepsilon^\alpha(\mu) - \varepsilon^\beta(\mu))}{16\pi\gamma R^5}}\frac{p}{\varepsilon^\alpha(\mu)} \qquad [19b]$$

(H has the meaning of the dimensionless electric dipole moment). Simultaneously, the specific boundary conditions given by Equation (10) can be rewritten in the form

$$\tilde{\Phi}^\alpha|_{\tilde{r}=0} = const, \qquad \tilde{\Phi}^\beta \underset{r'\to\infty}{\longrightarrow} -\tilde{r}x, \qquad [20a]$$

$$\tilde{\Phi}^\alpha \underset{r'\to 0}{\longrightarrow} \frac{x}{\tilde{r}^2}, \qquad \tilde{\Phi}^\beta \underset{r'\to\infty}{\longrightarrow} 0. \qquad [20b]$$

In view of the axial symmetry of the electric field, let us seek the solution to Equations (11) and (7) in the form of expansion in the Legendre polynomials $P_m(x)$ (m is the order of polynomial)

$$\tilde{r}(x) = \sum_{m=0}^{\infty}\tilde{d}_m P_m(x), \qquad [21]$$

$$\tilde{\Phi}^\alpha(\tilde{r}, x) = \sum_{m=0}^{\infty}\tilde{b}_m\tilde{r}^m P_m(x),$$

$$\tilde{\Phi}^\beta(\tilde{r}, x) = -\tilde{r}x + \sum_{m=0}^{\infty}\frac{\tilde{a}_m}{\tilde{r}^{m+1}}P_m(x), \qquad [22a]$$

$$\tilde{\Phi}^\alpha(\tilde{r}, x) = \frac{x}{\tilde{r}^2} + \sum_{m=0}^{\infty}\tilde{b}_m\tilde{r}^m P_m(x),$$

$$\tilde{\Phi}^\beta(\tilde{r}, x) = \sum_{m=0}^{\infty}\frac{\tilde{a}_m}{\tilde{r}^{m+1}}P_m(x), \qquad [22b]$$

where the dimensionless coefficients $\tilde{d}_m$, $\tilde{a}_m$, and $\tilde{b}_m$ are determined as

$$\tilde{d}_m = d_m/R, \qquad \tilde{a}_m = \frac{1}{\Psi R^{m+1}}a_m, \qquad \tilde{b}_m = \frac{R^m}{\Psi}b_m. \qquad [23]$$

Here d_m, a_m, and b_m are the dimensional coefficients of expansion of dimensional quantities $r(x)$, $\Phi^\alpha(r, x)$, and $\Phi^\beta(r, x)$ in the Legendre polynomials.

Expansions (22a,b) satisfy Equation (7) with the specific boundary conditions (20a,b), and we see after the substitution of Equation (21) and (22a,b) into Equations (12)–(14) that the initial problem is converted into a solution to the set of equations

$$g_i = 0, \qquad i = 1, 2, 3 \qquad [24]$$

for dimensionless coefficients $\tilde{d}_m$, $\tilde{a}_m$, and $\tilde{b}_m$ simultaneously with the equation obtained after substitution of Equation (21) into Equation (17). How many independent parameters may we use seeking the solution to the problem? From the point of thermodynamics we have 3 independent variables of state for the system under consideration. These 3 thermodynamic degrees of freedom include temperature T, chemical potential μ (or the radius R), and the electric field intensity $\vec{E}$ (or associated quantity). The temperature is assumed to be fixed, and this leaves only 2 thermodynamic degress of freedom. These degrees correspond to dimensionless parameters G and H in Equation (14). However, in view of the dimensionless form of Equation (17), only one of these parameters can be determined independently. Nevertheless, return to the dimension variables in the solution restores the second independent parameter. For example, if we have found G as a function of H in the course of solving Equation (24), then in order to reveal the dependence of radius R on the characteristic of the electric field, we need to specify $P_0^\alpha - P_0^\beta$, i.e., to specify the chemical potential. It should be noted in view of Equation (13) that the relative dielectric permittivity ε also remains an independent parameter of the dimensionless problem (although ε is not a thermodynamic degree of freedom).

THE NUMERICAL ALGORITHM FOR THE PROBLEM

The symmetry of Equation (14) and the antisymmetry of the specific boundary conditions (20a,b) in x yield

$$d_{2m+1} = a_{2m} = b_{2m} = 0 \qquad (m = 0, 1, 2, \dots). \qquad [25]$$

Multiplying Equation (24) by the Legendre polynomials $P_m(x)$, $m = 0, 1, 2, \dots$, and integrating over x from -1 to 1, taking into account the symmetry of the problem, we obtain

$$F_1^m = \int_0^1 g_1(x) P_{2m+1}(x)\, dx = 0, \qquad [26]$$

$$F_2^m = \int_0^1 g_2(x) P_{2m+1}(x)\, dx = 0, \qquad [27]$$

$$F_3^m = \int_0^1 g_3(x) P_{2m}(x)\, dx = 0. \qquad [28]$$

Equation (17) can be rewritten in the similar form

$$F_4 = \int_1^0 \tilde{r}^3 P_0(x)\, dx - 1 = 0. \qquad [29]$$

Thus we have an infinite set of nonlinear algebraic equations for coefficients a_{2m+1}, b_{2m+1}, and d_{2m} ($m = 0, 1, 2, \dots$). Let us cut off the series in Equations (21)–(22b) at the Legendre polynomial $P_N(x)$ of order N. Correspondingly, we will consider only those Equations (26)–(28) where the order of the Legendre polynomials does not exceed N. In this way the problem is transformed into a solution of a finite set of nonlinear algebraic equations for coefficients a_{2m+1}, b_{2m+1}, and d_{2m} ($m = 0, 1, 2, \dots, 2m+1 \le N$) with three external parameters G, H, and ε. As was noted at the end of the last section, only 2 of these parameters are independent.

We will solve the set of equations by the Newton iteration procedure (Dennis and Schnabel 1983). Let us specify any 2 parameters among G, H, and ε. The parameter that stays unspecified we will designate as t. Now we can introduce vector $\vec{X} = (\{d_{2m}\}, \{b_{2m+1}\}, \{a_{2m+1}\}, t)$ and the residual vector $\vec{F} = (\{F_1^m\}, \{F_2^m\}, \{F_3^m\}, F_4)$ ($m = 0, 1, 2, \dots, 2m + 1 \le N$). Thus the set of equations can be written in the form $A\vec{X} = 0$, where A is the nonlinear operator corresponding to the truncated set of Equations (26)–(29). Then the iteration procedure is formulated as follows. As a first step, we have the appropriate approximation $\vec{X}_0$ for the droplet shape, electric potential, and variable t and calculate $\vec{F}_0 = A\vec{X}_0$ and the matrix $J_{ij}^0 = \partial(A\vec{X})_i / \partial X_j$ at $\vec{X} = \vec{X}_0$. With the help of the equation $J^0\vec{s}_0 = -\vec{F}_0$, we find the next approximation $\vec{X}_1 = \vec{X}_0 + \vec{s}_0$ and then repeat the whole process starting from $\vec{X}_1$ until the required accuracy is achieved.

Let us say a few words about the initial approximation. At $H = 0$ the droplet shape is spherical with radius R. As follows from Equations (14), (15), and (24), we have $G = 1$ in this case, but we need to determine a_k and b_k also. We can do this by solving Equations (26) and (27) for the sphere $\tilde{r} = 1$. Thus we have an exact solution for Equation (26)–(29) for $H = 0$. Designating $t = G$, increasing H at fixed ε, and choosing the solution for the preceding value of H as the initial approximation, we can obtain a solution for an arbitrary electric field. However, starting from some value H^*, such a procedure may appear ineffective. As an example of this situation, one may consider the case when H^* is close to the point where $|\partial G / \partial H| \to \infty$ (the thermodynamic instability point). It is convenient to designate $t = H$ in this situation and replace the variation of parameter H by the variation of parameter G. In some cases such an approach allows us to pass over the thermodynamic instability points and distinguish these points from the instability points of the numerical method itself, which correspond to zeros of matrix J_{ij}.

If the parameters H and ε are chosen as independent, then the solution for variable t gives the value for G. Taking into account Equations (15) and (16), we are now able to find $P_0^\alpha - P_0^\beta$ as a function of the equivalent sphere radius R and the electric field intensity. Assuming the liquid in the droplet to be incompressible, one can obtain the expression for the chemical potential of condensate. Counting off the chemical potential from the value for the vapor-liquid equilibrium with planar interface, expressing it in thermal energy units kT (k is the Boltzmann constant),

and denoting the obtained dimensionless quantity as b_R, we have

$$b_R = G\frac{2\gamma}{RkT\rho^\alpha}, \qquad [30]$$

where ρ^α is the number of molecules per unit volume of bulk liquid. This expression determines the chemical potential of condensate as a function of R. For the number ν of molecules inside the droplet of incompressible liquid we have

$$\nu = \frac{4\pi R^3}{3}\rho^\alpha. \qquad [31]$$

Thus the dependence of the chemical potential of condensate in the droplet on ν can be easily found from (30) and (31).

Let us note now that the expression for the work of droplet formation in the electric field can be written as

$$F_\nu = -b\nu + \frac{\gamma A}{kT} + \frac{W_{el}}{kT}, \qquad [32]$$

where b is the dimensionless vapor chemical potential defined similarly (321) to b_R (we assume that the vapor chemical potential is kept the same as in the absence of the field (Warshavsky and Shchekin 1996, 1999; Shchekin and Varshavskii 1996), A is the surface area of the droplet, and W_{el} is the free energy of droplet polarization. The surface area is determined by the solution for the droplet profile, while W_{el} is derived from the expression for the potential of reaction field at the location of the field sources. Thus the expressions for A and W_{el} can be written as (Warshavsky and Shchekin 1996, 1999; Shchekin and Varshavskii 1996)

$$A = 2\pi\int_0^1 \sqrt{\left[r^2 + (1-x^2)r_x^2\right]}\, r\, dx, \qquad [33]$$

$$W_{el} = -\frac{1}{2}a_1\varepsilon^\beta(\mu)E_\infty, \qquad [34a]$$

$$W_{el} = \frac{1}{2}b_1 p. \qquad [34b]$$

In this way both quantities, $\gamma A/kT$ and W_{el}/kT, that play an important role in thermodynamics of nucleation can be independently found from the results of our numerical approach.

Let us say a few words about the accuracy control during the computations. One can use 2 methods here. The first method is the control of the value of $|\vec{F}|$ until it becomes sufficiently small. The second method is the control of the quantity

$$\sqrt{\int_0^1 \left(g_1^2 + g_2^2 + g_3^2\right) dx}.$$

Both methods become equivalent as $N \to \infty$, however, the interpretation of the methods is essentially different at finite N. The first method shows the quality of the reduced set of equations, while the second method serves for evaluation of waived terms. Approaching the region of instability of the numerical procedure, the estimate obtained by the first method stays small in spite of the fact that the number of iterations considerably increases. At the same time, the estimate obtained by the second method starts to grow. This fact may be considered as the evidence that we have found a good solution for the reduced set of equations, but, getting closer to the instability region, the solution begins to deviate notably from a solution for a nonreduced set of equations.

RESULTS FOR THE EXTERNAL UNIFORM FIELD

The effects of an external uniform electric field on the shape and stability of a dielectric droplet are mostly worked out (Cheng 1984; Cheng and Chaddock 1984; Basaran and Scriven 1989; Wohlhuter and Basaran 1993; Warshavsky and Shchekin 1996, 1999) and from that point the case of the external uniform field may serve as a control example for a general approach to an axisymmetric electric field in nucleation.

The results of the numerical procedure described in the last section for the case of external uniform electric fields (specified by Equations (19a), (22a), and (34a)) are illustrated in Figures 1–4. Curve 1 in Figures 1a and 1b shows the dependence of droplet aspect ratio $\beta(\beta \equiv \tilde{r}(x = 1)/\tilde{r}(x = 0))$ on the dimensionless parameter

$$\delta^2 = 9\frac{\varepsilon - 1}{(\varepsilon + 2)^2}H^2 \qquad [35]$$

for 2 values of relative dielectric permittivity ε: $\varepsilon = 10$ (for the dichlorethane) and $\varepsilon = 78$ (for the water). At small deviations of a droplet shape from the sphere, parameter δ has a geometrical meaning of the eccentricity of a prolate (along the direction of the field intensity) spheroid. This behavior is confirmed by the results of the perturbation theory for small δ^2 (Warshavsky and Shchekin 1996, 1999), where the following asymptotic forms were obtained for the droplet shape, the chemical potential, and the surface and the polarization contributions to the work of droplet formation:

$$r(x) = R\left[\left(1 - \frac{1}{45}\delta^4\right) + \left(\frac{1}{3}\delta^2 + \frac{79}{315}\delta^4 - \frac{4}{5(\varepsilon+2)}\delta^4\right) \times P_2(x) + \frac{26}{315}\delta^4 P_4(x)\right], \qquad [36]$$

$$b_R = \frac{2\gamma}{kT\rho^\alpha R}\left(1 - \frac{1}{3}\frac{\varepsilon+2}{\varepsilon-1}\delta^2 - \frac{4}{45}\delta^4\right), \qquad [37]$$

$$\frac{\gamma A}{kT} = \frac{4\pi\gamma R^2}{kT}\left(1 + \frac{2}{45}\delta^4\right), \qquad [38]$$

$$\frac{W_{el}}{kT} = -\frac{4\pi\gamma R^2}{kT}\left(\frac{2}{9}\frac{\varepsilon+2}{\varepsilon-1}\delta^2 + \frac{4}{45}\delta^4\right) \qquad [39]$$

(for the sake of convenience the equations were rewritten in slightly changed form in comparison to Warshavsky and Shchekin (1999)).

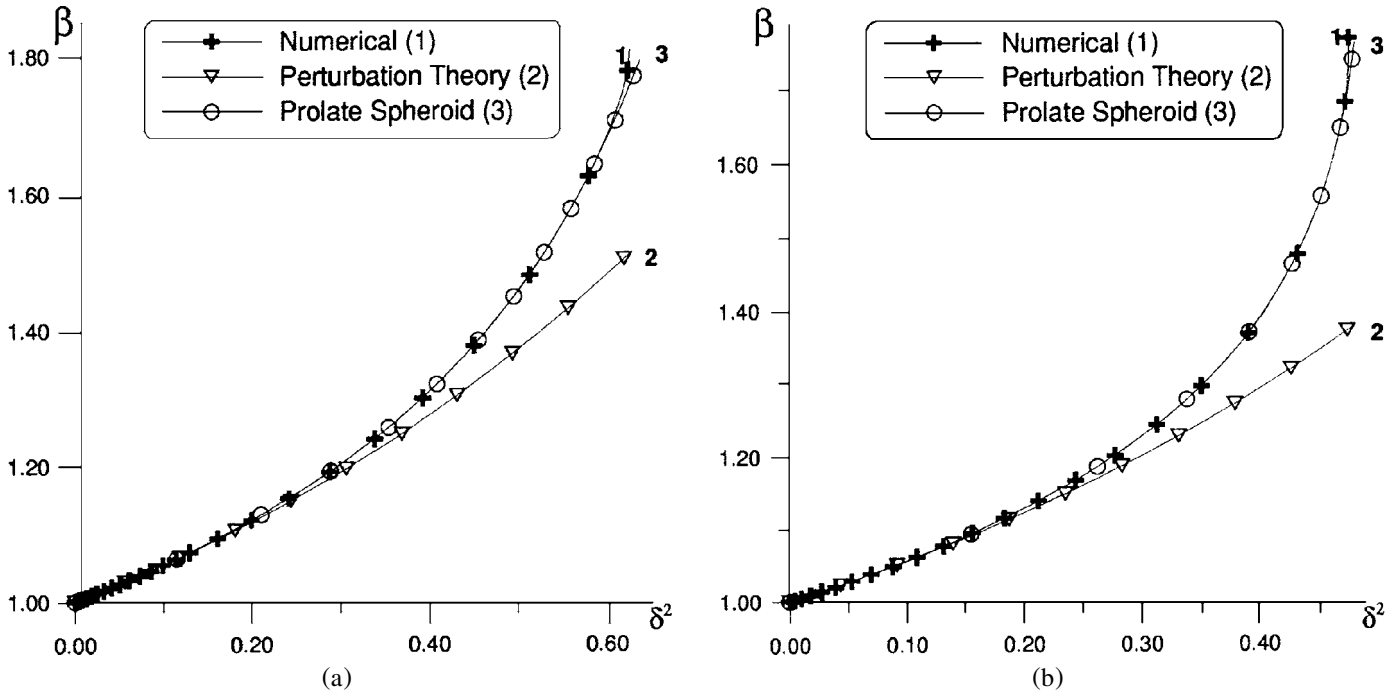

Figure 1. The dependence of aspect ratio β of the droplet equilibrium shape on the dimensionless parameter δ^2 associated with the intensity of the uniform external electric field (see Equations (35) and (19a)) at 2 values of relative dielectric permittivity $\varepsilon = 10$ (a) and $\varepsilon = 78$ (b). Curves 1, 2, and 3 depict the numerical, the perturbation theory (see Equation (36)) and the prolate spheroid results, respectively.

The dependence of the droplet aspect ratio β on δ^2, which corresponds to Equation (36), is depicted in Figures 1a and 1b by curve 2. As one can see, there is good agreement between curves 1 and 2 for $\delta^2 \leq 0.4$. The increasing deviation between curves 1 and 2 for $\delta^2 > 0.4$ is not surprising because the deformation of the droplet from the sphere cannot be considered as small at these values of δ^2. Curve 3 in Figures 1a and 1b shows the droplet aspect ratio for the droplet having a form of the prolate spheroid within the whole interval of variation of δ^2 (Cheng 1984). In fact, asymptotic expansion in Equation (36) demonstrates that, with the accuracy up to terms of order of δ^4, the shape of the droplet deviates from the prolate spheroid. Nevertheless, curves 1 and 3 are in very good agreement. This agreement is slightly distorted only in the vicinity of the turning point at $\delta^2 = 0.4776$ in Figure 1b. As is well known (Cheng 1984; Cheng and Chaddock 1984; Basavan and Scriven 1989; Wohlhuter and Basaran 1993), the turning point marks the loss of droplet shape stability: shapes before and beyond the turning point correspond to stable and unstable equilibrium, respectively. It was found in Basaran and Scriven (1989) and Wohlhuter and Basaran (1993) by Galerkin's method of weighted residuals that the turning point of the conducting droplet is reached at $\delta^2 = 0.46$. There is no such turning point in Figure 1a. This confirms the observation (Cheng 1984; Wohlhuter and Basaran 1993) that the turning point in the curve of the aspect ratio versus the intensity of the uniform external electric field disappears at $\varepsilon < 20$. In order to pass the turning point in our numerical investigation at $\varepsilon = 78$, we used the "switching" from independent parameter H to independent parameter G in the vicinity of the turning point as it was noted in the last section.

Let us evaluate the electric field intensity at which the considered effect on the droplet shape is significant. As follows from Equations (35) and (19a), the intensity of the electric field equals $E_\infty = 2.75$ MV/m in the case of water droplets ($\varepsilon^\alpha = 78$, $\gamma = 73$ mN/m) in the vapor-air surroundings ($\varepsilon^\beta = 1$) at $R = 2.5 \cdot 10^{-4}$m and at $\delta^2 = 0.4776$ (the turning point). This intensity is less than the air breakdown limit, which equals 3 MV/m. But the electric field intensity grows up to $E_\infty = 43.5$ MV/m with decreasing the droplet radius to $R = 1$ μm. In the case of dichlorethane droplets ($\varepsilon^\alpha = 10$, $\gamma = 31$ mN/m) in the vapor-air surroundings ($\varepsilon^\beta = 1$) at $\delta^2 = 0.6$, the electric field intensity equals $E_\infty = 2.6$ MV/cm and $E_\infty = 40.8$ MV/m at $R = 2.5 \cdot 10^{-4}$m and $R = 1$ μm, respectively. Thus the external electric field is able to considerably affect the growth of supercritical drops in nucleation, while the formation of small subcritical and critical droplets remain undisturbed.

Figure 2 shows the dependence of parameter G, which is related in view of Equation (30) to the chemical potential of the droplet substance on δ^2 at $\varepsilon = 78$. Curve 1 represents the results of our numerical approach; curve 2 plots $b_R kT\rho^\alpha R/2\gamma$ according to Equation (37). As one can see, the agreement of both curves is rather good within the whole interval for δ^2 before the turning point.

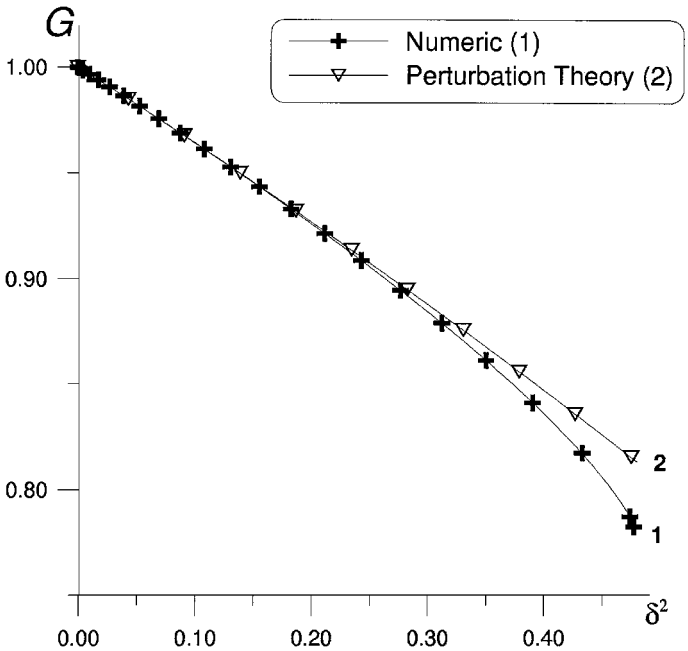

Figure 2. The dependence of the droplet dimensionless chemical potential G on the dimensionless parameter δ^2 associated with the intensity of the uniform external electric field (see Equations (35) and (19a)) at $\varepsilon = 78$. Curves 1 and 2 depict the numerical and the perturbation theory (see Equation (37)) results, respectively.

Figures 3a and 3b show the dependence of the relative surface, $\bar{W}_s \equiv \gamma A/4\pi\gamma R^2$, and polarization, $\bar{W}_{el} \equiv W_{el}/4\pi\gamma R^2$, contributions to the work of the droplet formation. Curves 1 and 2 demonstrate the results of the numerical approach and the results following from Equations (38) and (39), respectively. Curve 3 shows these contributions for the droplet having the form of a prolate spheroid. As follows from Cheng (1984), we have in this case

$$\bar{W}_s = \frac{\beta^{-2/3}}{2} + \frac{\beta^{1/3} e_s^{-1}}{2} \arcsin e_s, \qquad [40]$$

$$\bar{W}_{el} = -\frac{2}{27}\frac{(\varepsilon+2)^2}{(\varepsilon-1)}\frac{\delta^2}{1+(\varepsilon-1)\tau}. \qquad [41]$$

Here

$$\tau \equiv \left[\left(1-e_s^2\right)/2e_s^3\right]\{\ln[(1+e_s)/(1-e_s)] - 2e_s\}, \qquad [42]$$

$e_s = \sqrt{1-\beta^2}$ is the eccentricity of the spheroid. The equilibrium values for β and e_s are determined from equation $\partial F_v/\partial\beta|_{R,\delta} = 4\pi\gamma R^2 \partial(\bar{W}_s + \bar{W}_{el}/\partial\beta|_\delta = 0$.

As one can see, curves 1 and 3 almost coincide in Figures 3a and 3b. At the same time the deviation of curve 2 from curve 1 increases with increasing δ^2, but for $\bar{W}_{el}$ curve 2 lies above curve 1, while for $\bar{W}_s$ curve 2 lies below curve 1. Figure 4 depicts the behavior of sum $\bar{W}_s + \bar{W}_{el}$ as a function of δ^2. Agreement of curve 1 obtained from the numerical procedure and curve 2 obtained from Equations (38) and (39) is rather good, and it is possible to say about the compensation of deviations in $\bar{W}_s$ and $\bar{W}_{el}$. Because sum $\bar{W}_s + \bar{W}_{el}$ is the only part in the free energy of droplet formation that depends on δ^2 (for a fixed vapor chemical potential), we can conclude that the expression for the free energy of droplet formation determined by the perturbation theory is valid within a wide interval of δ^2.

RESULTS FOR THE INTERNAL NONUNIFORM FIELD OF HETEROGENEOUS NUCLEUS WITH AN ELECTRIC DIPOLE MOMENT

The results of the numerical procedure described earlier for the case of the internal nonuniform field of heterogeneous condensation nucleus with an electric dipole moment (specified by Equations (19b), (20b), (22b), and (34b)) are illustrated in Figure 5–10. Curve 1 in Figure 5 shows the dependence of droplet aspect ration $\beta(\beta \equiv \tilde{r}(x=0)/\tilde{r}(x=1))$ on the dimensionless parameter

$$\eta^2 = 9\frac{\varepsilon(\varepsilon-4)}{(\varepsilon+2)^2}H^2 \qquad [43]$$

at $\varepsilon = 10$ (for dichlorethane). At small deviations of the droplet shape from the sphere, parameter η has a geometrical meaning of the eccentricity of an oblate (along the direction of the dipole moment of the condensation nucleus) spheroid. This behavior is confirmed by the results of the perturbation theory for small η^2 (Shchekin and Varshavskii 1996). The following asymptotic forms were obtained in Shchekin and Varshavskii (1996) for the droplet shape, the chemical potential, and the surface and the polarization contributions to the work of droplet formation

$$r(\theta) = R\left\{1 - \frac{\eta^2}{3}P_2 - \eta^4 \times\left[\frac{1}{45} + \left(\frac{194}{315} - \frac{21}{5}\frac{(\varepsilon+10/7)\varepsilon^2}{(\varepsilon-4)(\varepsilon+2)(3\varepsilon+4)}\right)P_2 + \left(\frac{2}{21} + \frac{16}{15}\frac{\varepsilon}{(3\varepsilon+4)(\varepsilon-4)}\right)P_4\right]\right\}, \qquad [44]$$

$$b_R = \frac{2\gamma}{RkT\rho^\alpha}\left(1 - \frac{2}{3}\frac{\varepsilon+2}{\varepsilon-4}\eta^2 + \frac{8}{45}\eta^4\right), \qquad [45]$$

$$\frac{\gamma A}{kT} = \frac{4\pi\gamma R^2}{kT}\left(1 + \frac{2}{45}\eta^4\right), \qquad [46]$$

$$\frac{W_{el}}{kT} = \frac{4\pi\gamma R^2}{kT}\left(\frac{4}{9}\frac{\varepsilon+2}{\varepsilon-4}\eta^2 - \frac{4}{45}\eta^4\right) + f_W, \qquad [47]$$

where f_W is the work of wetting of the heterogeneous condensation nucleus by the bulk liquid (f_W is not important for our analysis because it does not contribute to the energy barrier of nucleation (Shchekin and Varshavskii 1996)). For the sake of convenience, Equations (44)–(47) were rewritten in a slightly changed form in comparison to Shchekin and Varshavskii (1996)

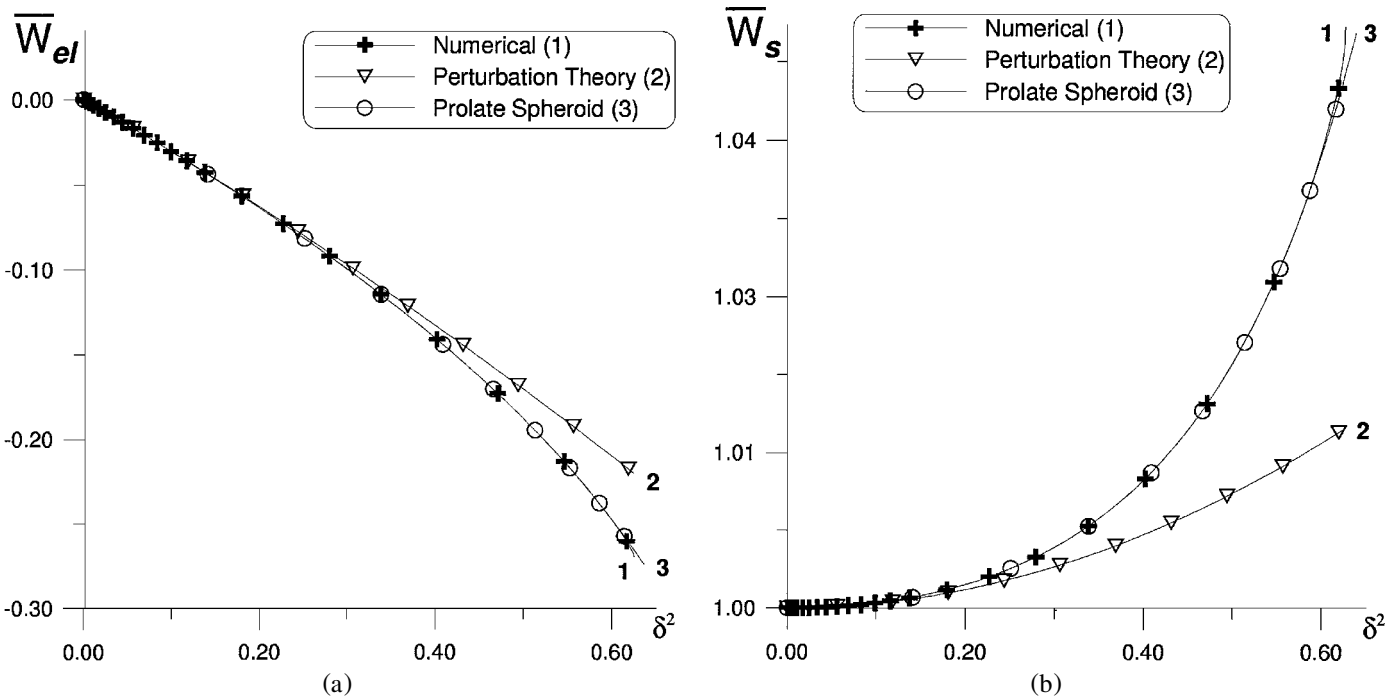

Figure 3. The dependence of the polarization contribution to the work of droplet formation $\bar{W}_{el}$ and the work of surface formation $\bar{W}_s$ on the dimensionless parameter δ^2 associated with the intensity of the uniform external electric field (see Equations (35) and (19a)) at $\varepsilon = 10$. Curves 1, 2, and 3 depict the numerical, the perturbation theory (see Equations (38) and (39)), and the prolate spheroid (see Equations (40)–(42)) results, respectively.

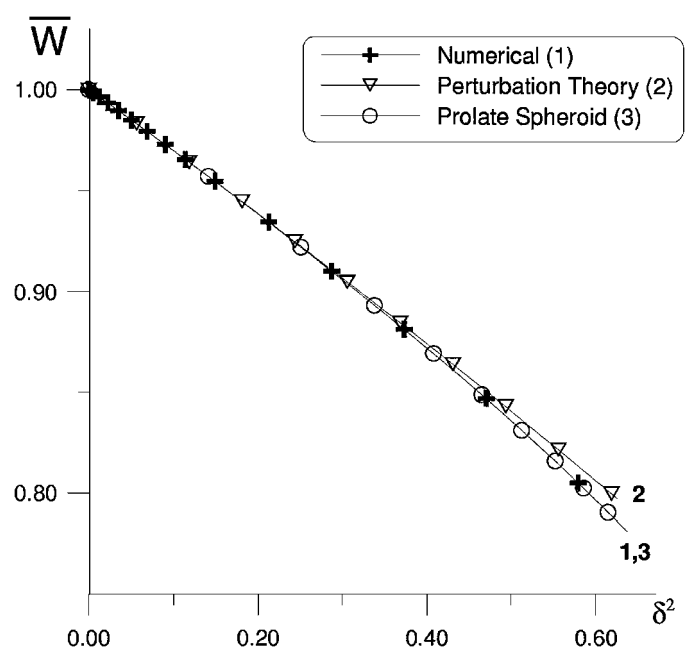

Figure 4. Sum $\bar{W}_s + \bar{W}_{el}$ as a function of the dimensionless parameter δ^2 associated with the intensity of the uniform external electric field (see Equations (35) and (19a)) at $\varepsilon = 10$. Curves 1, 2, and 3 depict the numerical, the perturbation theory, and the prolate spheroid results, respectively.

and we correct misprints that occurred in formulas (48) and (49) Shchekin and Varshavskii (1996).

The plot of droplet aspect ratio versus η^2 that corresponds to Equation (44) is depicted in Figure 5 by curve 2. As one can see, good agreement between curves 1 and 2 is only for rather small values of $\eta^2 : \eta^2 \lesssim 0.1$ (this region is shown in detail in the complementary figure). The increasing deviation between curves 1 and 2 for $\eta^2 > 0.1$ reflects the asymptotic character of expansion (44). It should be noted that the curve corresponding to the term of order of η^2 in Equation (44) lies at $\eta^2 > 0.1$ above curve 1 in Figure 5, while curve 2 lies below curve 1.

Figure 6 shows the dependence of parameter G, which is related in view of Equation (30) to the chemical potential of droplet substance, on η^2. Curve 1 represents the results of our numerical approach, and curve 2 plots $b_R kT\rho^\alpha R/2\gamma$ according to Equation (45). As one can see, the agreement of both curves is good even for high values of η^2. Thus we can conclude that Equation (45) is valid in a very wide range of η^2, considerably exceeding the range of validity for Equation (44).

The behavior of the chemical potential b_R as a function of dimensionless variable R/R_*, where $R_* \equiv 2\gamma/kT\rho^\alpha$, is depicted in Figure 7. The dipole moment was taken as

$$p = \sqrt{(16/9)R_*^5 \pi \gamma \varepsilon^\alpha(\mu)}$$

with $\varepsilon = 10$. The dependence shown in Figure 7 is typical for heterogeneous nucleation (it is similar, for example, to the

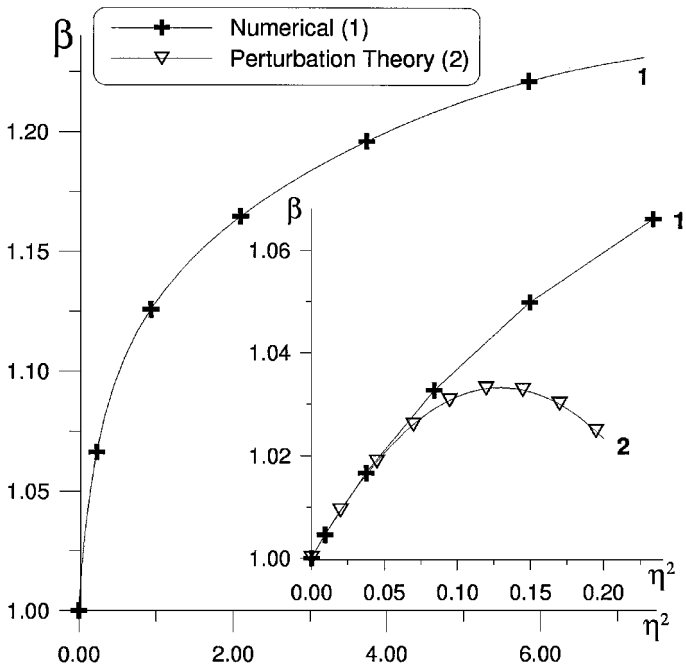

Figure 5. The dependence of aspect ratio β of the droplet equilibrium shape on the dimensionless parameter η^2 associated with the dipole moment of the heterogeneous condensation nucleus (see Equations (43) and (19b)) at $\varepsilon = 10$. Curves 1 and 2 depict the numerical and the perturbation theory (see Equation (44)) results, respectively.

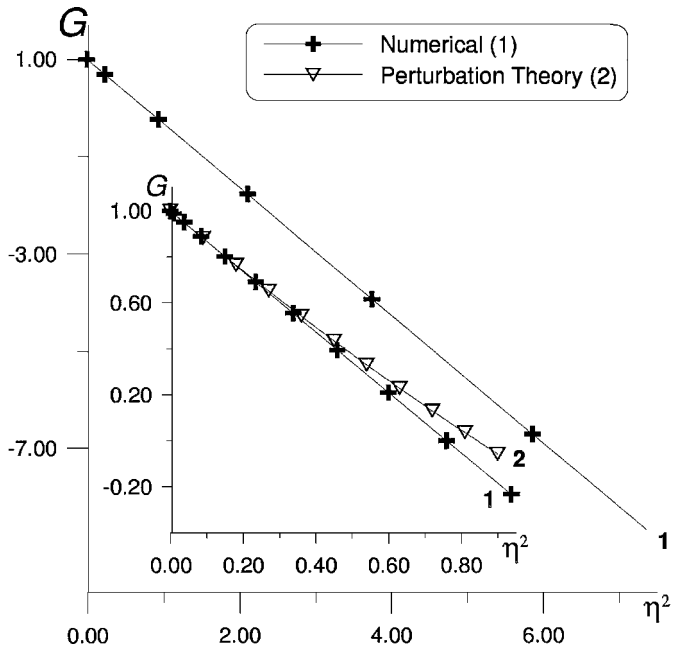

Figure 6. The dependence of the droplet dimensionless chemical potential G on the dimensionless parameter η^2 associated with the dipole moment of the heterogeneous condensation nucleus (see Equations (43) and (19b)) at $\varepsilon = 10$. Curves 1 and 2 depict the numerical and the perturbation theory (see Equations (30), (45)) results, respectively.

behavior of the chemical potential of a droplet in ion-induced nucleation).

Figures 8a and 8b show the dependence of the relative surface, $\bar{W}_s$, and polarization, $\bar{W}_{el}$, contributions to the work of droplet formation. Curves 1 and 2 demonstrate the results of our numerical approach and the results following from Equations (46) and (47), respectively. Figure 9 shows the behavior of sum $\bar{W}_s + \bar{W}_{el}$ as a function of η^2. The deviations in the curves shown in Figures 8a, 8b, and 9 are similar to the deviations depicted in Figures 3a, 3b, and 4. Thus we again can make the conclusion about the mutual compensation of deviations in $\bar{W}_s$ and $\bar{W}_{el}$ in the expression for the work of droplet formation.

Figure 10 shows the droplet shape in dimensionless cylindrical coordinates $\tilde{z} = z/R$ and $\tilde{\rho} = \rho/R$ at rather high values of η^2: $\eta^2 = 6.83$. According to Equations (43) and (19b), such a high value of η^2 requires an extremely small droplet size and can not be achieved for any molecular dipole center. For instance, we obtain $R = 1.0$ Å for droplets of dichlorethane ($\varepsilon = 10$, $\gamma = 31$ mN/m) corresponding to $\eta^2 = 6.83$ with the water molecule as an electric dipole center ($p = 1.83$ D). Thus Figure 10 illustrates the tendency rather than an observable phenomenon.

DISCUSSION

Let us summarize the results of the investigation. The droplet profile in the uniform external electric field looks like a prolate

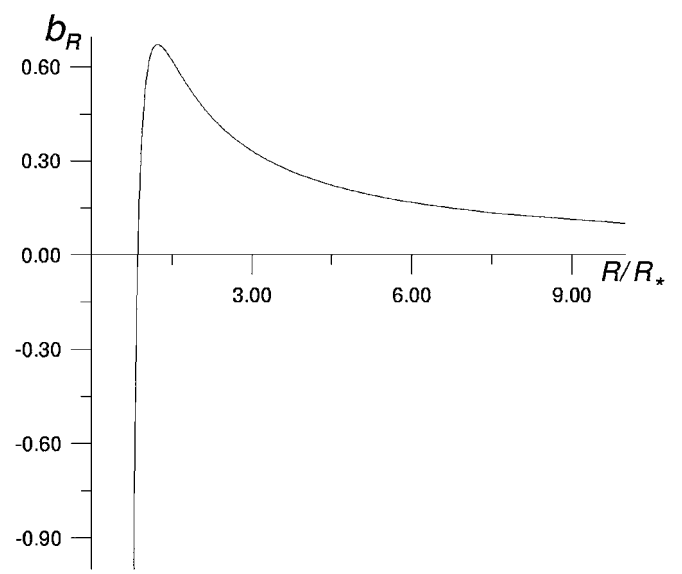

Figure 7. The dependence of the chemical potential of condensate in the dielectric droplet on the droplet size in the internal electric field of a dipole of the heterogeneous condensation nucleus. Here $R_* = 2\gamma/kT\rho^\alpha$ is the characteristic scale of the droplet size. The location of the maximum in the curve depends on dipole moment p, which was taken here as $p = (4/3) \cdot R_*^{5/2} \sqrt{\pi \gamma \varepsilon^\alpha(\mu)}$.

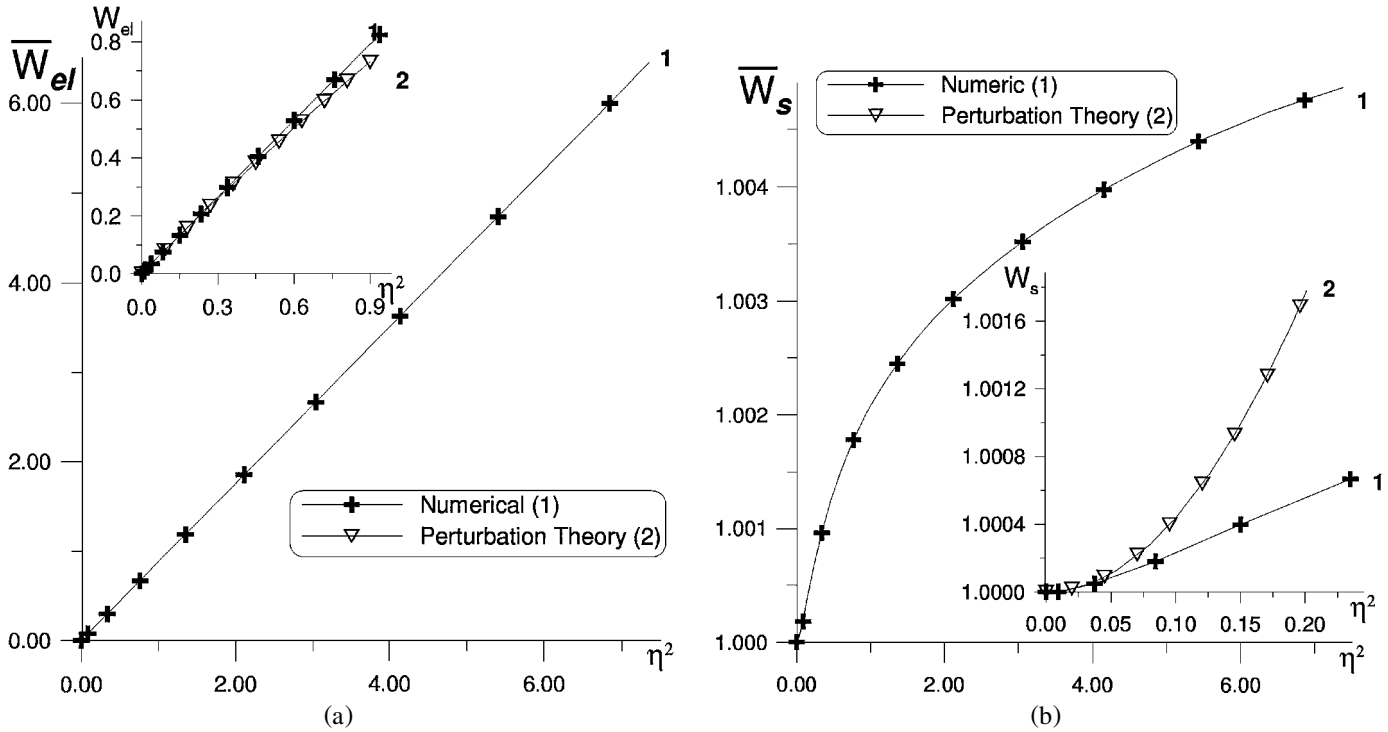

Figure 8. The dependence of the polarization contribution to the work of droplet formation $\bar{W}_{el}$ and the work of surface formation $\bar{W}_s$ on the dimensionless parameter η^2 associated with the dipole moment of the heterogeneous condensation nucleus (see Equations (43) and (19b)) at $\varepsilon = 10$. Curves 1 and 2 depict the numerical and the perturbation theory (see Equations (46), (47)) results, respectively.

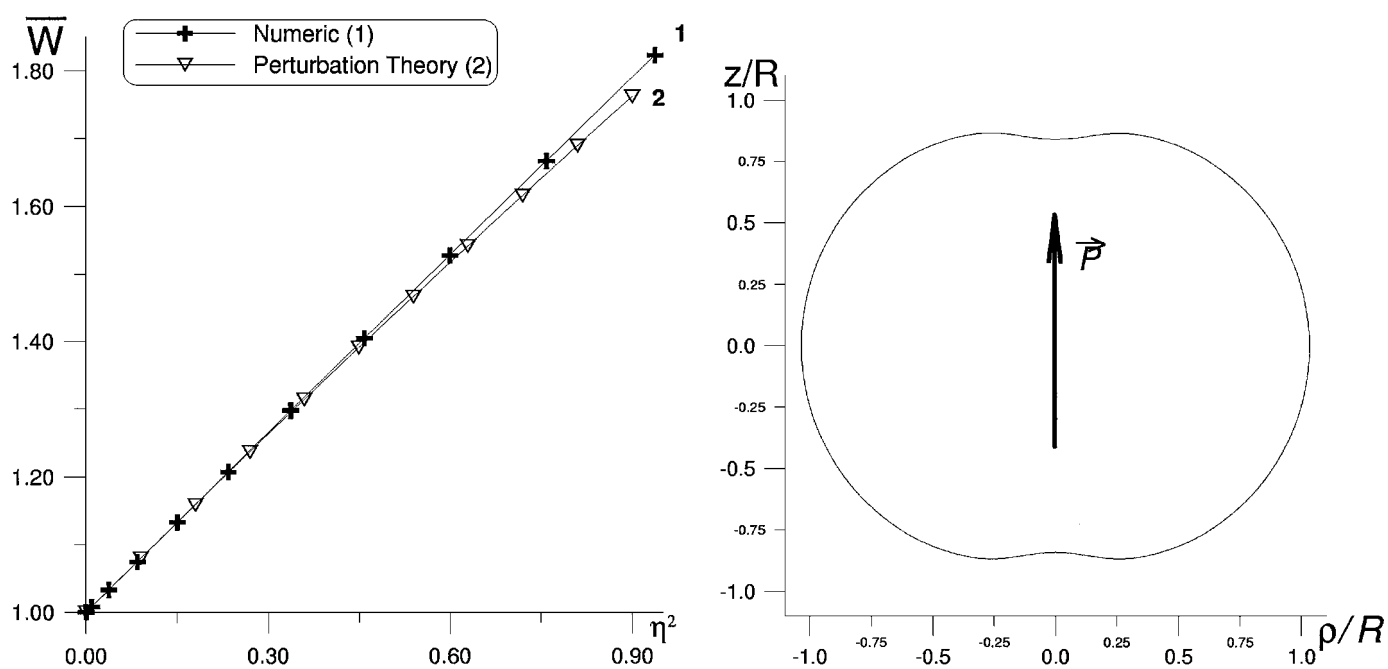

Figure 9. Sum $\bar{W}_s + \bar{W}_{el}$ as a function of the dimensionless parameter η^2 associated with the dipole moment of the heterogeneous condensation nucleus (see Equations (43) and (19b)) at $\varepsilon = 10$. Curves 1 and 2 depict the results of the numerical and the perturbation theory, respectively.

Figure 10. The shape of the droplet in the internal electric field of the dipole of the heterogeneous condensation nucleus at $\varepsilon = 10$, $G = -7.98$, $H = 1.35$, $\eta^2 = 6.83$, $\beta = 1.23$, $\bar{W}_{el} = 6.44$, and $\bar{W}_s = 1.00487$. The axis z is collinear with the dipole moment $\vec{p}$.

(along the field direction) spheroid for all values of parameter δ^2 until its critical value 0.4776. The droplet profile in the electric field of the dipole of the heterogeneous nucleus looks like an oblate (along the dipole moment direction) spheroid only for small values of parameter η^2 and transforms to the apple-like shape at large η^2.

Comparison of the thermodynamic results obtained by our numerical procedure to that of the perturbation theory shows in both considered cases the following: While the validity of the droplet profiles derived analytically is really limited to small deviations from the spherical shape, the region of validity of the formulas for the chemical potential and the free energy of droplet formation is much wider. The main reason for is that provided by the mutual compensation in the nonspherical and polarization contributions. The partial compensation of these contributions should take place even in the general case of an arbitrary electric field. The distortion of the spherical shape of the droplet in the axisymmetric electric field leads to decreasing of the polarization contribution to the free energy of droplet formation. Because the surface energy contribution is minimal for the sphere (with a fixed volume), the distortion of the spherical shape increases this contribution. In view of generating properties of the free energy of droplet formation in nucleation theory, the same conclusion stays valid for other nucleation characteristics.

REFERENCES

Basaran, O. A., and Scriven, L. E. (1989). *Phys. Fluids A* 1:799.
Cheng, K. J. (1984). *Phys. Lett.* 106A:403.
Cheng, K. J., and Chaddock, J. B. (1984). *Phys. Lett.* 106A:51.
Dennis, J. E., and Schnabel, R. B. (1983). *Numerical Methods for Unconstrained Optimization and Nonlinear Equation*, Prentice-Hall, Englewood Cliffs, NJ.
Holland, P. M., and Castleman, Jr., A. W., (1982). *J. Phys. Chem.* 86:4181.
Kuni, F. M., Shchekin, A. K., and Rusanov, A. I. (1984). *Colloid J. of the USSR* (English translation) 45:598.
Shchekin, A. K., and Varashavski, V. B. (1996). *Colloid J.* 58:564.
Warshavsky, V. B., and Shchekin, A. K. (1996). In *Fizika aerodispersnykh sistem (Physics of Aerodispersed Systems)*, 36:61 (in Russian).
Warshavsky, V. B., and Shchekin, A. K. (1999). *Colloids and Surfaces A: Physicochemical and Engineering Aspects* 148:283.
Wilson, C. T. R. (1900). *Phil. Trans.* 193A:289.
Wohlhuter, F. K., and Basaran, O. A. (1993). Effects of Physical Properties and Geometry on Shapes and Stability of Polarizable Drops in External Fields. *J. Magn. & Magn. Mater.*122:259.